Cycle generative adversarial network approaches to produce novel portable chest x-ray images for COVID-19 diagnosis

Daniel I. Morís, J. de Moura, J. Novo and M. Ortega

VARPA Group
Department of Computer Science
University of A Coruña

Table of Contents

Table of Contents

COVID-19: The Global Pandemic

- Coronavirus Disease 2019 (COVID-19) is an infectious disease caused by the novel coronavirus SARS-CoV-2.
- Due to its rapid spread, the COVID-19 was declared as a global pandemic by the WHO in March 11th, 2020.

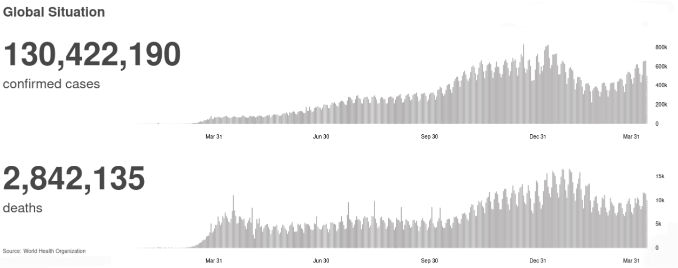

COVID-19

COVID-19

- It mainly affects the respiratory tissues.
- For the most severe cases, mechanical ventilation and ICU admission could be necessary.

World Health Organization

COVID-19 affects different people in different ways. Most infected people will develop mild to moderate illness and recover without hospitalization.

Most common symptoms:

- fever.
- dry cough.
- tiredness.

Serious symptoms:

- difficulty breathing or shortness of breath.
- chest pain or pressure.
- loss of speech or movement.

Chest X-ray image modality

- Chest X-ray image modality is a **well-established medical imaging technique**, widely used during the last decades for the **clinical diagnosis of common pulmonary diseases**.

Portable Chest X-ray devices

Portable Chest X-ray devices

- To control the COVID-19 spread, the cut of transmision chains is critical.
- To minimize the **risk of cross-contamination**, American College of Radiology recommends to use **portable chest X-ray machinery**.

Example of a common portable chest X-ray device capture.

Data scarcity problem

- **Data scarcity** is usually a problem in **medical imaging domains**.
- Due to the recent emergence of the COVID-19 disease, data scarcity is even **more critical** in this particular domain.

Example of chest X-ray images from a real clinical context

Cycle Generative Adversarial Networks (CycleGAN)

Cycle Generative Adversarial Networks (CycleGAN)

- This GAN architecture is able to perform an **image translation**.
- Powerful approach to **generate novel synthetic images**.

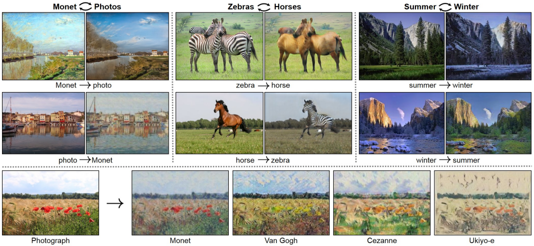

Unpaired Image-to-Image Translation using Cycle-Consistent Adversarial Networks (Zhu *et al.*, 2017)

COVID-19 detection in chest X-ray images

- Many works have addressed the automatic COVID-19 detection in chest X-ray images.
- However, a great part of these works used the **COVID-19 Image Data Collection dataset**.
- In that dataset, most of the images were captured with **fixed X-ray devices**, that provide **good quality** and detail **in contrast with portable devices**.
- Most of the images have **no reference about the used acquisition device**.

Objectives

Objectives

- Obtain a method able to artificially increase the dimensionality of a chest X-ray dataset
  - Help expert clinicians in the task of COVID-19 diagnosis
  - Unsupervised strategy
  - No need for paired data
  - Augmentation of three different classes
  - Dataset composed of images acquired with a portable chest X-ray device of a real clinical context

Table of Contents

Table of Contents

CHUAC Dataset

- The images were provided by the Radiology Service of the Complexo Hospitalario Universitario A Coruña (CHUAC).
- The chest X-ray images were captured with portable devices during the first peak of the pandemic.

Dataset

CHUAC Dataset

- **Capture devices:** Agfa dr100E GE and Optima Rx200
- **600 images**
  - **200 healthy cases** (*i.e.* without pleural or pulmonary diseases)
  - **200 pathological cases** (with pulmonary pathologies others than COVID-19)
  - **200 COVID-19** genuine cases

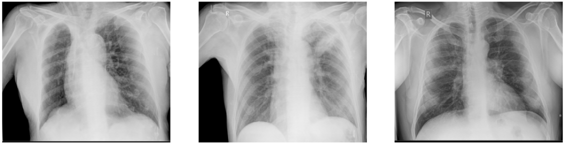

a) b) c)

Representative examples of the CHUAC dataset. (a) Healthy case. (b) Pathological case. (c) COVID-19 case.

Table of Contents

Methodology

- The methodology is divided in two main steps
  - Data augmentation
  - Screening

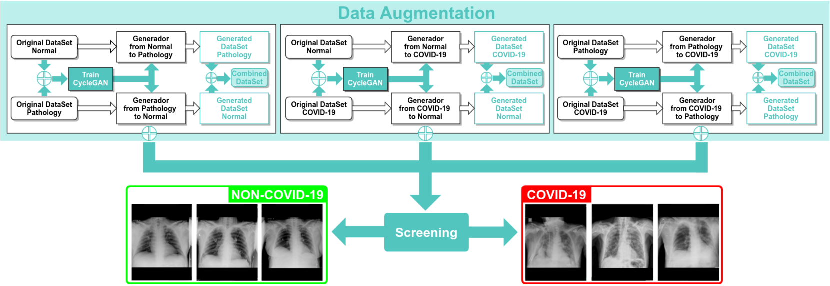

Overview of the proposed methodology.

Methodology: 1st step - Data Augmentation

- 3 different scenarios are considered.
  - **Healthy vs Pathological**
  - **Healthy vs COVID-19**
  - **Pathological vs COVID-19**

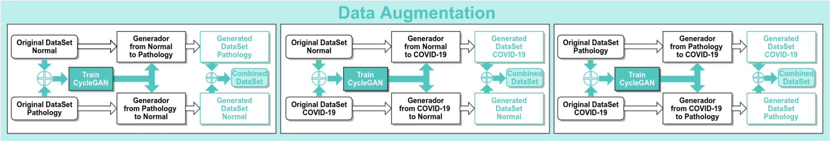

Methodology: 1st step - Data Augmentation

Network architecture and training details

- **All the available images** are used to train the CycleGAN models.
- CycleGAN configuration: **ResNet with 9 residual blocks** architecture for the **generative model**.
- Trained during **250 epochs** with **Adam** algorithm (**constant learning rate** of $\alpha = 0{,}0002$).
- **Mini-batch size** of 1.

Methodology: 1st step - Data Augmentation

1st scenario

- Translation from **Healthy** to **Pathological** and **vice versa**.
  - **1st pathway:** the model should add pathological structures.
  - **2nd pathway:** the model should remove pathological structures.

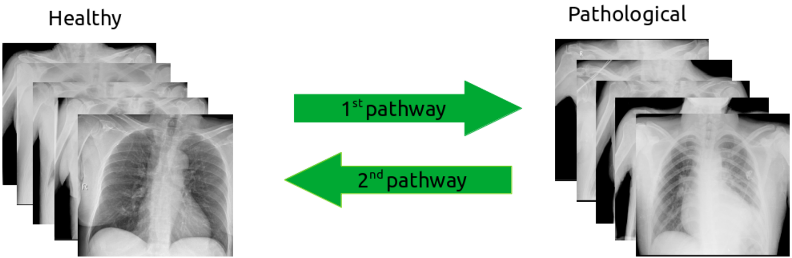

2nd scenario

- Translation from **Healthy** to **COVID-19** and **vice versa**.
  - **1st pathway:** the model should add COVID-19 affectation structures.
  - **2nd pathway:** the model should remove COVID-19 affectation structures.

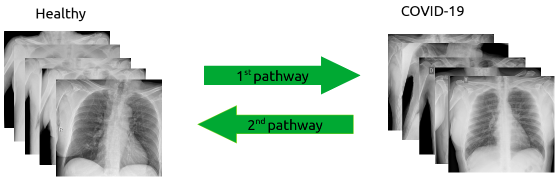

Methodology: 1st step - Data Augmentation

3rd scenario

- Translation from **Pathological** to **COVID-19** and **vice versa**.
  - **1st pathway:** the model should remove COVID-19 affectation to add pathological structures of other pulmonary diseases.
  - **2nd pathway:** the model should remove pathological structures of pulmonary diseases others than COVID-19 to add COVID-19 affectation.

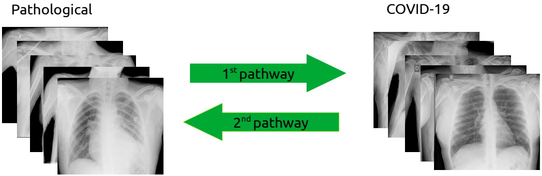

Methodology: 2nd step - COVID-19 Screening

Screening

- We perform screening tasks to validate the separability among generated samples.
- The last experiment proves the suitability of the oversampled dataset for a COVID-19 screening.

Methodology: 2nd step - COVID-19 Screening

Network architecture and training details

- A **Dense Convolutional Network Architecture (DenseNet)** was used (particularly, a **DenseNet-161**).
- The input data is **randomly partitioned** in three sets.
  - **60 %** of samples for **training**.
  - **20 %** of samples for **validation**.
  - **20 %** of samples for **test**.

Methodology: 2nd step - COVID-19 Screening

Network architecture and training details

- The used model was **pretrained** on the **ImageNet dataset**.
- **Cross-entropy** as loss function.
- The model was trained **200 epochs**, with the **Stochastic Gradient Descent Algorithm (SGD)**.
    - **Constant learning rate** of $\alpha = 0{,}01$.
    - **Mini-batch size** of 4.
    - **First-order momentum** of 0.9.
    - The training process is **repeated 5 times**.

Table of Contents

Results - Experiments

Experimental validation

- In order to validate our proposal, **4 experiments were conducted**.
- The **first 3 experiments** validate the **degree of separability** among the **generated images** for the possible scenarios.
  - **Healthy vs Pathological**
  - **Healthy vs COVID-19**
  - **Pathological vs COVID-19**
- The **fourth experiment** was performed to analyze the **COVID-19 screening** with the **oversampled dataset**.
- For the experimental validation, 4 different metrics are used: **Precision**, **Recall**, **F1-Score** and **Accuracy**.

List of conducted experiments

- **1st experiment** - Separability among healthy and pathological generated samples
- **2nd experiment** - Separability among healthy and COVID-19 generated samples
- **3rd experiment** - Separability among pathological and COVID-19 generated samples
- **4th experiment** - COVID-19 screening using the original dataset with oversampling

Separability among **healthy** and **pathological generated** samples

- Test results demonstrate a **proper separability** among the healthy and pathological generated images.
- We achieved a **0.9375** of **global accuracy** for **test**.

Cases	Precision	Recall	F1-Score
Healthy	0.92	0.95	0.94
Pathological	0.95	0.93	0.94

Separability performance among healthy and pathological generated samples.

Results - 2nd experiment - Healthy vs COVID-19

Separability among **healthy** and **COVID-19 generated** samples

- Test results demonstrate a **proper separability** among the healthy and COVID-19 generated images.
- We achieved a **0.8687** of **global accuracy** for **test**.

Cases	Precision	Recall	F1-Score
Healthy	0.84	0.90	0.87
COVID-19	0.90	0.84	0.87

Separability performance among healthy and COVID-19 generated samples.

Separability among **pathological** and **COVID-19 generated** samples

- Test results demonstrate a **proper separability** among the pathological and COVID-19 generated images.
- We achieved a **0.9375** of **global accuracy** for **test**.

Cases	Precision	Recall	F1-Score
Pathological	0.91	0.98	0.94
COVID-19	0.97	0.90	0.93

Separability performance among pathological and COVID-19 generated samples.

Results - 4th experiment - Oversampled dataset

- The correct classification and misclassification ratios show acceptable results.
- Particularly, the correct classification ratio was a **0.9328** for the **Healthy/Pathological** case (**NON COVID-19**) and a **0.9098** for the **COVID-19** samples.

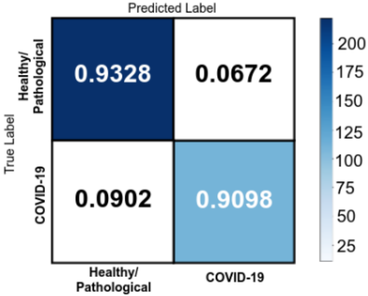

Confusion matrix for the 4th experiment on the test set.

Results - Synthetic image generation

Image translation

It is clearly visible that the images obtained using the CycleGAN have **remarkable and well-synthesized differences in pulmonary regions**.

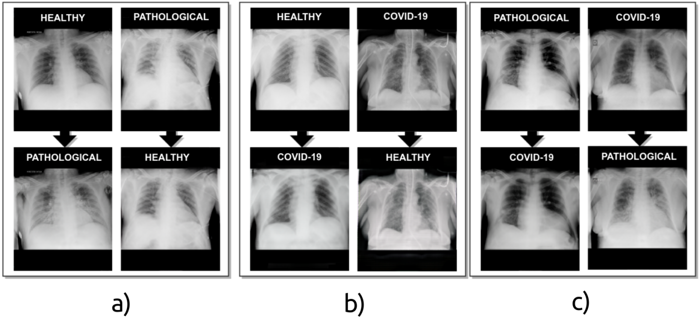

Examples of images generated by the CycleGAN architecture. (a) 1st scenario, Healthy vs Pathological. (b) 2nd scenario, Healthy vs COVID-19. (c) 3rd scenario, Pathological vs COVID-19.

Table of Contents

Conclusions

Conclusions

- We propose **novel and fully automatic approaches** to **artificially increase the size** of a chest X-ray dataset used for **COVID-19 diagnosis**.
- The **CycleGAN** was used in order to generate **synthetic images** in **3 complementary scenarios**.
- **Satisfactory results** were obtained despite the **low quality and detail of the portable acquisition devices** used to build the input dataset

Future Works

Future Works

- This oversampling strategy can be proved to improve the performance of a particular final task.
- This methodology could be exploited in the context of other pulmonary pathologies or other medical imaging domains.

Acknowledgements

Acknowledgements

This research was funded by Instituto de Salud Carlos III, Government of Spain, DTS18/00136 research project; Ministerio de Ciencia e Innovación y Universidades, Government of Spain, RTI2018-095894-B-I00 research project; Ministerio de Ciencia e Innovación, Government of Spain through the research project with reference PID2019-108435RB-I00; Consellería de Cultura, Educación e Universidade, Xunta de Galicia, Grupos de Referencia Competitiva, grant ref. ED431C 2020/24; Axencia Galega de Innovación (GAIN), Xunta de Galicia, grant ref. IN845D 2020/38; CITIC, Centro de Investigación de Galicia ref. ED431G 2019/01, receives financial support from Consellería de Educación, Universidade e Formación Profesional, Xunta de Galicia.

Thanks for your attention!